

COMMISSIONING AND INITIAL EXPERIMENTS ON NDCX-II*

S. M. Lidia[#], T. Schenkel^{##}, W. G. Greenway, K. Murphy, T. Schenkel, C. D. Weis, W. L. Waldron, Lawrence Berkeley National Laboratory, Berkeley, CA 94720, U.S.A.

Abstract

The Neutralized Drift Compression Experiment (NDCX-II) is a new induction accelerator facility designed to facilitate user experiments in high energy density laboratory physics, intense beam physics, and materials processing and testing with intense, pulsed ion beams. The facility has completed the initial commissioning phase of its injector, 27-cell solenoid transport lattice, induction accelerator modules and non-neutral pulse compression section. Space-charge-dominated Li^+ beams carrying 20-50 nC have been generated from the 133 kV pulsed, ~ 1.0 microsecond (FWHM), 65-mA injector, and compressed to 20-30 ns with 0.75-1.3 A peak currents and amplification factors of 10-20. We report results of non-neutral beam compression and transport studies to generate variable ion beam fluences on to solid targets. We also report on studies of dose rate effects in pulsed ion implantation and on the recombination dynamics of radiation-induced defects in semiconductors using the NDCX-II Li^+ beam.

INTRODUCTION

The NDCX-II facility [1, 2] was constructed between July 2009 and December 2012. Commissioning results of the source and injector systems has already been reported [3]. The induction accelerator modules with pulsed, 2-3 T solenoid magnet transport were added in several stages (5-cell, 11-cell, 27-cell) to facilitate the integration of diagnostic and controls systems [4]. The 27-cell beamline configuration is shown in Fig. 1, with schematic representation indicating the position of the active induction cell modules, diagnostic cells, injector and end station.

Each cell is instrumented with a pulse solenoid for transport. The original complement of beam diagnostics for commissioning included a movable end station complemented with a Faraday cup, slit and slit-cup pairs, and scintillator viewable through downstream flange window. A pepper-pot mask and dedicated scintillator were added later, with the removal of the slit/slit-cup pairs. Other non-interceptive beam diagnostics included 6 capacitive plate beam position monitors at the diagnostic cell locations, solenoid current transformers, and accelerator cell voltage resistive monitors. This level of beam instrumentation was sufficient for initial beam transmission studies and beam quality measurements.

* This work is supported by the Director, Office of Science, Office of Fusion Energy Sciences, of the U.S. Department of Energy under Contract No. DE-AC02-05CH11231.

[#]smlidia@lbl.gov, ^{##}T_Schenkel@LBL.gov

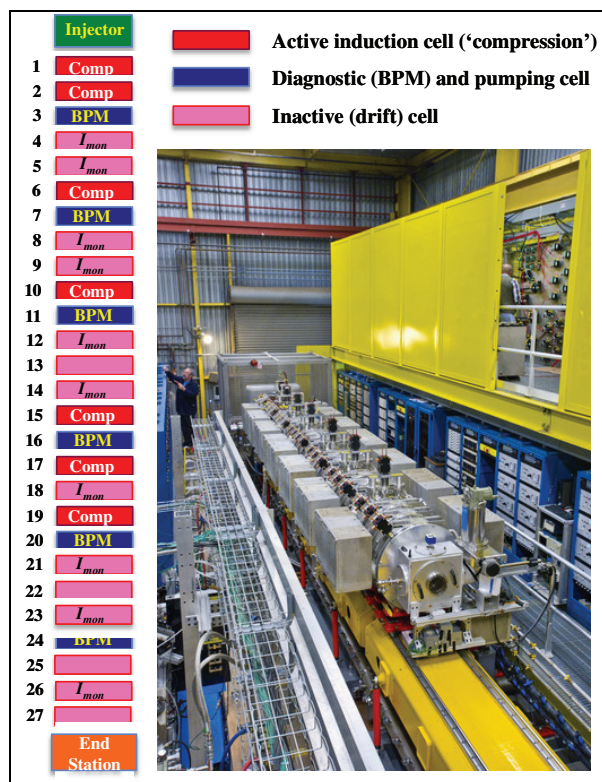


Figure 1: NDCX-II beamline and schematic.

ENHANCED DIAGNOSTICS AND COMMISSIONING STRATEGY

The modular beamline is built up from 21 identical induction cells and 6 diagnostic cells. For these commissioning exercises, only 7 of the induction cells are active, with the remaining inactive cells providing drift length for longitudinal compression. We utilized an additional 10 inactive cells as reciprocal inductive current monitors. The drive matching circuits for these cells were modified to provide a $\sim 5\Omega$ termination, and measured L/R response times were in the range of 1.6 – 2.2 μs .

These additional current diagnostics increased the spatial resolution of time-of-flight measurements along the beamline, and permitted determination of velocity and beam energy to within accepted error margins. Furthermore, interpolation of the beam arrival time and beam pulse duration to the active induction cell positions permits fine tuning of the accelerating voltage waveform amplitude and delay, enabling optimization of the bunch compression process and tailoring of the magnetic solenoid lattice.

LONGITUDINAL COMPRESSION AND ACCELERATION

The 7 active induction cells function to impress a time-varying energy (or velocity) ramp on the beam and, with the additional drift lengths between them, to allow the beam to compress longitudinally with concurrent increase in the peak current. The injector and induction cell voltage waveforms are shown in Fig. 2 for a particular tune of delays and amplitudes.

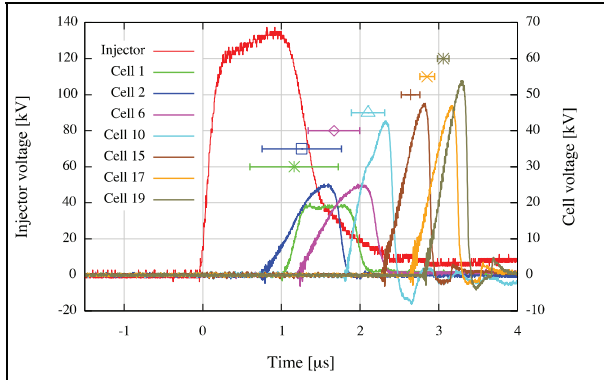


Figure 2: Injector and induction cell voltages. Interpolated beam arrival times and pulse durations are indicated.

Beam line charge density profiles and beam current profiles are measured with the BPMs and inductive current monitors, respectively. The current waveforms are shown in Fig. 3.

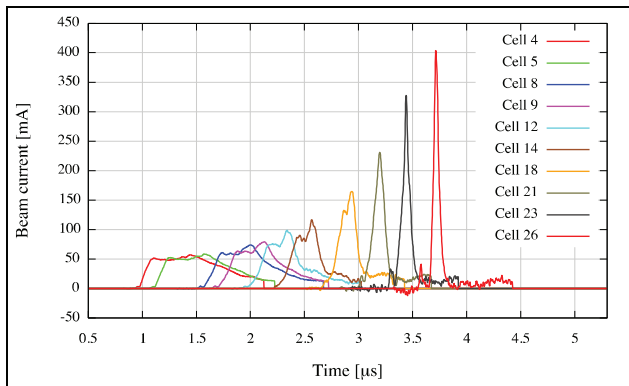


Figure 3: Evolution of beam current profile.

Time-of-flight calculations based on the arrival times of the pulse leading edge at the monitoring stations is used to generate a profile of the beam velocity and energy evolution through the machine. The peak current, average beam energy, and pulse duration (FWHM) are shown in Fig. 4.

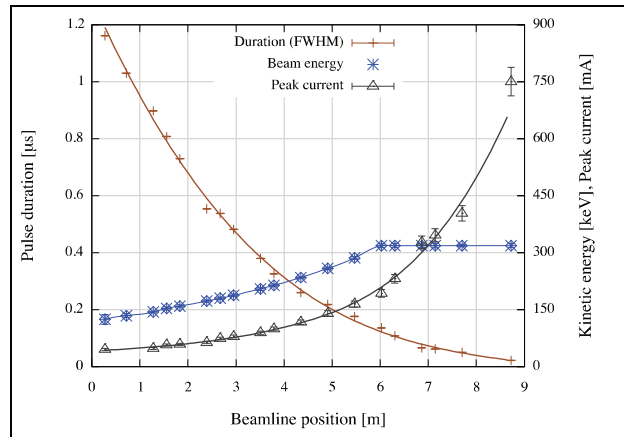


Figure 4: Evolution of longitudinal beam parameters.

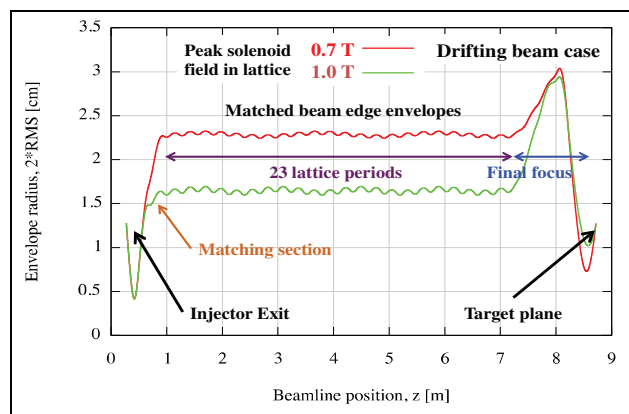


Figure 5: Solenoid transport tune classes for 135 keV, 65 mA drifting beam.

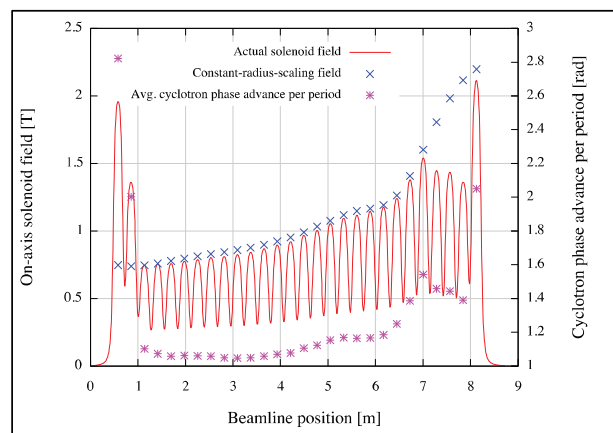


Figure 6: Solenoid field profile match to evolving beam current and energy.

BEAM TRANSPORT

Several classes of solenoid focusing lattice tunes were examined for beam matching and transmission in the drifting (i.e. not accelerator or compressed) case. Simple space-charge dominated envelope simulations were performed and are shown in Fig. 5.

These tune classes provide a basis for tuning the compressed pulse case. Using the field scaling $B^2 \sim I_{pk}/v_{avg}$, where I_{pk} and v_{avg} are the peak currents and average bunch velocity, respectively, we retune the solenoid field (Fig. 6) to maintain constant beam radius along the accelerator.

BEAM EMITTANCE AND FLUENCE

At the target plane, a scintillator captures the beam transverse profile, while a pepper-pot is used to measure the 4D phase space distribution. The last solenoid is scanned to vary the beam envelope and convergence angle. The resultant variation in the radius, peak fluence, and emittances is shown in Fig. 7 for the compressed beam case (Table 1).

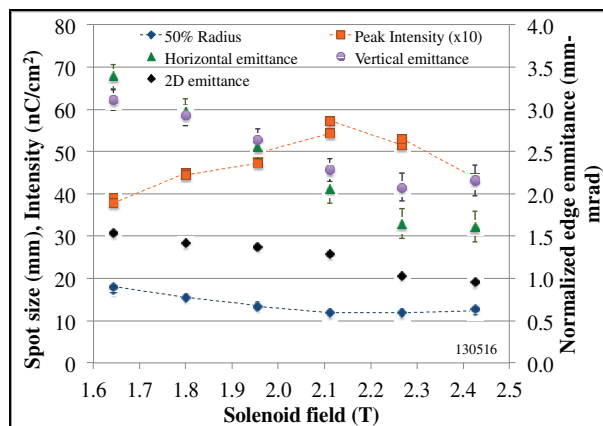


Figure 7: Peak intensity and emittances at target plane.

Table 1: Target Plane Beam Parameters

	Drifting	Compressed
Final energy (keV)	135	315
Peak current (mA)	65	760
Pulse length, FWHM (ns)	450	20
50% beam radius (mm)	5.1	11.8
Average fluence (mJ/cm ²)	3	0.84
Peak intensity (kW/cm ²)	8.8	88

INITIAL TARGET EXPERIMENTS

Intense, short ion beam pulses enable pump-probe type experiments to access the multi-scale (ps to many seconds) dynamics of radiation induced defects in materials [5, 6]. Using NDCX-II, we are conducting studies to examine the pulse length and peak fluence dependence on lattice defect generation and recovery in single crystal silicon and metals. First, we irradiated single crystal silicon (100) samples and performed *ex situ* SIMS (Secondary Ion Mass Spectrometry) analysis of Li ion depth profiles [5]. Here, damage built-up during ion implantation shots reduces the probability for ions to channel along high index crystal directions. When varying dose rates ($\sim 0.1 - 50$ mA/cm²) and pulse lengths ($\sim 20 - 500$ ns), we saw evidence for defect recombination on a 100 ns time scale.

In the next series of experiments we utilize a thin (1- μ m) single crystal silicon (100) membrane to intercept the beam. The membrane thickness is chosen to block the randomly scattered ions while allowing the channeled ion flux to pass. A fast Faraday cup (FFC) on the downstream side of the membrane is used to collect the transmitted ions with a time resolution of a few ns. The effect of

pulse duration and peak fluence on transmitted beam is shown in Fig. 8. In the long pulse/lower fluence (137 keV, 640 ns, 6 nC) case, the transmitted flux profile reproduces the control case without the Si membrane, indicating low effective angles for the uncompressed beam. In the short pulse case (261 keV, 40 ns, 2.2 nC), the transmitted ion current profile deviates significantly from the control case. For the tuning conditions of this 40 ns shot, ions in the pulse peak are mostly absorbed in the membrane, indicating effective beam angles of a few degrees, while trailing ions later in the pulse transmit the membrane, indicating beam angles $< 1^\circ$. The critical angle for channeling of ~ 300 keV Li⁺ ions in Si (100) is about 1° . Ion transmission tracking provides *in situ* feedback for tuning of effective beam angles. For the short pulse tune in Fig. 8, ions in the peak generate defects (vacancies and interstitials) and the disordered lattice is probed by ions that arrive later on channeling trajectories. For the relatively low dose rates present in the shots shown in Figure 8, we see no evidence for damage built-up. Dose rates will be increased 10 to 50 fold in experiments with shorter (~ 15 ns), more intense (~ 40 nC) pulses. Tuning of pump-probe type ion beam pulses shapes [6] and implementation of auxiliary diagnostics will enable unprecedented access to multi-scale defect dynamics in materials.

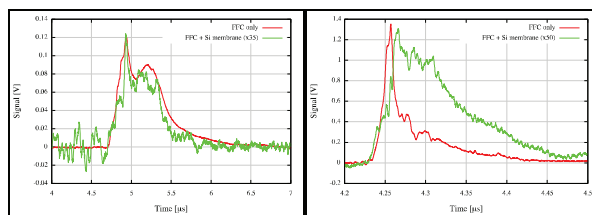


Figure 8: Current traces for a single 640 ns long (left) and 40 ns short pulse (right), with (green) and without (red) Silicon membrane target in front of the FFC.

SUMMARY

We have implemented diagnostics and tuning techniques to produce a variety of target plane conditions on NDCX-II, with unneutralized pulse compression ratios of 10-20 for high permeance ($\sim 10^{-2}$) beams. The measured beam quality matches numerical predictions. We present results from experiments that utilize the unique short pulse capabilities of NDCX-II.

REFERENCES

- [1] A. Friedman et al., Phys. Plasmas 17 (2010) 056704.
- [2] W.L. Waldron, NIM A (2013), in press.
<http://dx.doi.org/10.1016/j.nima.2013.05.063>
- [3] P.A. Seidl et al., PR-STAB 15 (2012) 040101.
- [4] S. Lidia et al., IPAC 12 Proceedings, MOEPPB005.
- [5] T. Schenkel et al., NIM B (2013),
<http://dx.doi.org/10.1016/j.nimb.2013.05.074>
- [6] A. Froideval et al., J. Nucl. Mater. 416 (2012) 242.